*Avrupa Bilim ve Teknoloji Dergisi*
*Özel Sayı, S. 82-92, Ekim 2019*

**Araştırma Makalesi**

www.ejosat.com ISSN:2148-2683

*European Journal of Science and Technology*
*Special Issue,, pp. 82-92, October 2019*

**Research Article**

# Localization and Point Cloud Based 3D Mapping with Autonomous Robots

Selya Açıkel[1*], Ahmet Gökçen[2]

[1] Institute of Engineering and Science, Iskenderun Technical University, Turkey (ORCID: 0000-0001-5443-6713)
[2] Department of Computer Engineering, Iskenderun Technical University, Turkey (ORCID: 0000-0002-7569-5447)

(This publication has been presented orally at HORA2019 congress.)

(First received 1 August 2019 and in final form 22 October 2019)

(**DOI:** 10.31590/ejosat.636389)

**ATIF/REFERENCE:** Açıkel, S. & Gökçen A. (2019). Localization and Point Cloud Based 3D Mapping with Autonomous Robots. *European Journal of Science and Technology*, (Special Issue), 82-92.

**Abstract**

In this study, localization and environment mapping application is aimed with an autonomous robot. A new algorithm is presented to scan a larger area, to produce faster and more accurate results. The mapping process is intended not to be affected by environmental movements. It can be used in military areas to gain manpower in the mine area or to model the environment in virtual reality applications. In autonomous robot design, the horizontal and vertical angle values of the Lidar Lite V3 are provided by two servo motors. A four-wheeled car model was used. Ultrasonic sensors are placed on the front, right and left surfaces of the robot, Raspberry Pi 3 and Pi Camera was placed on top. It is seen that the moving average filter removes the noise generated on the map. The Lidar Lite V3 was able to take measurements at longer distances. Noise generation is prevented by motion detection algorithm. It can be used in interior space mapping, environment modeling, virtual reality applications, military areas, mining sector and graphic applications. In outdoor mapping, it can be used to create a map of an area of 40 meters in diameter. The mapping process was performed as close to the actual values by using the moving average filter and the Lidar Lite V3. The mapping process with the motion detection system is paused and actual position data are obtained using GPS.

**Keywords:** Mapping, localization, SLAM, Moving Average Filter, Lidar.

# Otonom Robotlarla Lokalizasyon ve Nokta Bulutu Tabanlı 3B Haritalama

**Öz**

Bu çalışmada otonom bir robot ile çevre haritalaması ve konum takibi yapılması amaçlanmıştır. Daha geniş bir alanın taranması, daha hızlı ve doğru sonuçların üretilmesi amacıyla yeni bir algoritma sunulmuştur. Haritalama işleminin ortam hareketlerinden etkilenmemesi amaçlanmıştır. Askeri alanlarda, maden alanında insan gücünden kazanç sağlamak veya sanal gerçeklik uygulamalarında ortam modeli çıkarmak amacıyla kullanılabilmektedir. Otonom robot tasarımında iki adet servo motor ile Lidar Lite V3'e yatay ve düşey açı değerleri verilmiştir. Dört tekerlekli bir araba modeli kullanılmıştır. Robotun ön, sağ ve sol yüzeylerine birer ultrasonik sensör ve üzerine Raspberry Pi 3 yerleştirilmiştir. Hareketli ortalamalar filtresinin haritada oluşan gürültüleri giderdiği görülmüştür. Lidar Lite V3 ile daha uzak mesafelerden ölçüm alınabilmiştir. Hareket algılama algoritması sayesinde gürültü oluşumu engellenmiştir. Pratikte iç mekan haritalamada, ortam modellemede, sanal gerçeklik uygulamalarında, askeri alanlarda, maden sektöründe ve grafik uygulamalarında kullanılabilir. Dış mekan haritalamada ise kırk metre çapında bir alanın haritasını oluşturmakta kullanılabilir. Haritalama işlemi,

[1] Corresponding Author: Institute of Engineering and Science, Iskenderun Technical University, Turkey, ORCID: 0000-0001-5443-6713, selyaacikel@gmail.com

hareketli ortalamalar filtresi ve Lidar Lite V3 kullanılarak gerçek değerlere en yakın şekilde gerçekleştirilmiştir. Hareket algılama sistemi ile haritalama işlemi duraklatılmıştır ve GPS kullanılarak gerçek konum verileri elde edilmiştir.

**Anahtar Kelimeler:** Haritalama, Lokalizasyon, SLAM, Hareketli Ortalamalar Filtresi, Lidar.

# 1. Introduction

With the rise and emerging of technologies, autonomous robots have become indispensable in human life. As in many areas, autonomous robots are used for mapping. In an environment where an autonomous robot does not have knowledge, the problem of mapping the environment and finding its own position is referred to in the literature as Simultaneous Localization and Mapping (SLAM) (Dissanayake, Newman, Durrant-Whyte, Clark & Csorba, 2000; Altuntaş, Uslu, Çakmak, Amasyalı, & Yavuz, 2017). The SLAM problem was first mentioned in 1986 at the IEEE Robotics and Automation Conference (Durrant-Whyte & Bailey, 2006). The most important material used to solve the SLAM problem is the scanners, cameras or distance sensors used to scan the environment. The materials directly affects the amount of noise in the generated map. Noise is a factor that reduces the ability of the system to predict. In order for the system to produce the results that are closest to reality, images should be cleaned as much as possible from noise. Since the 1990s, probabilistic methods have been used to eliminate noise (Thrun, 2002). Some commonly used probabilistic filters are Kalman Filter, Particle Filter and Popular Expectation Maximization. Most of the three-dimensional mapping with distance sensors uses point cloud topology. The mapping with point cloud is realized by combining numerous points and forming meaningful shapes. Rusu, R. et al. in 2008, based on the densities of the clustered points, they obtained successful results using the MLESAC (Maximum Likelihood Estimation Sample Consensus) algorithm for identifying objects from point clouds (Rusu, Marton, Blodow, Dolha, Beetz, 2008).

Sensors that make point measurements are used to create point clouds. The ultrasonic sensors, which were created by the French physicist Paul Langevin and measuring the distance with sound waves, were first introduced in 1917 (Graff, 1981). Infrared sensors measure distance based on the intensity of the infrared light they emit into their field of view. Today, devices that produce the most accurate results are laser distance sensors that do not require over-calculation. Lidar sensors, which are a kind of laser distance sensors and operate with radar logic, are high-range and low-error sensors (Fowler, 2000).

The autonomous robot needs to record his movements step by step in order to map his environment and also to determine his own position. It should be able to make certain calculations in each new movement and have information about the current moment. Various materials can be used to determine the position of the robot. GPS sensors, motors with encoders, GYRO sensors or compass sensors are some of the materials that can be used for motion and location tracking. GPS modules are not preferred for indoor mapping because they are inefficient in closed environments.

There are many studies in the literature on mapping with autonomous robots. Kurt Z. et al. used an infrared sensor as a distance sensor and suggested the Sequential Monte Carlo method, one of the particle filter applications, to reduce noise in the image. He successfully applied one of the statistical estimation methods to SLAM problems (Kurt, 2007).

In 2010, Ankışhan H. and Efe M. compared the results of simultaneous positioning and mapping of the square root odorless and square root difference from the Kalman Filters to those obtained from the Extended Kalman Filter and produced an alternative solution by saving the margin of error and time spent (Ankışhan & Efe, 2010).

In 2013, Golestan et al. by integrating the moving average filter into phase-locked loops, it has carried out a study to increase the accuracy of synchronization in grid-connected applications. They designed two different methods and compared their performance. In one of the methods, the success rate of the moving averages filter was higher than the other. In the second method, it was observed that the performance decreased depending on the frequency (Golestan, Ramezani, Guerrero, Freijedo & Monfared, 2013).

One of the problems encountered in SLAM problems is the motion estimation. The movements, coordinates and position of the autonomous robot reduce the calculation quality. In 2015, Carlone L. et al. suggested Exposure Graph Optimization based on nonlinear estimation methods such as Gauss and Newton in their estimation of rotation. They have succeeded in minimizing the errors caused by the movement of the autonomous vehicle (Carlone, Tron, Daniilidis, & Dellaert, 2015).

In 2017, Ramli et al. they have combined the molecular vision sensor with the Lidar Lite V3 in order to allow an UAV to move away from the obstacles, thus increasing the robustness and accuracy of the system. The UAV's obstacle prevention system has been also successful in textureless obstacles too (Ramli, Shamsudin & Legowo, 2017).

In 2018, Lee, K. et al. have worked on a pole star model and have made a study that the direction finding problem will be solved in the case of an object or structure that is to be noticed from everywhere such as pole star in the environment to be mapped. They proposed the Direction Landmark-based SLAM (DLSLAM) algorithm to detect the pole star model they called Direction Landmark (DL) and determine the direction accordingly (Lee, Ryu, Nam & Doh, 2018).

Hosseinzadeh M. et al. made a study that transforms the point sets of the environment mapped with an autonomous robot into meaningful objects with deep learning methods. By recognizing the objects previously taught, the robot provided more information about the environment. (Hosseinzadeh, Latif & Reid, 2018).

In this study, a solution was made to the SLAM problem in closed environments by measuring the distance with the Lidar Lite V3 integrated on the autonomous robot. The data has been received from the Lidar sensor is shown in 3D in the OpenGL supported desktop application with Point Cloud topology through the moving average filter. Unlike the literature, the errors that may occur in rotation and other movements have been resolved by means of processing some data received from a digital compass sensor and encoders integrated into the wheels of the autonomous vehicle. The GPS module on the autonomous robot is used to show the real coordinates of the environment to be mapped. The data obtained from the symmetrical three points of the environment are combined to display all the surfaces of the objects in the environment. Co-ordination of all processes is provided by Raspberry Pi 3. In order to reduce the errors in measurement by detecting the movement of the objects measured in the distance during measurement, motion detection was done with OpenCV supported image processing algorithms on the images taken from the camera placed on Raspberry.

# 2. Material and Method

## 2.1. Materials

### *2.1.1. Lidar Lite V3*

The Lidar Lite V3 is a laser distance sensor with a wavelength of 905nm. It is capable of measuring a maximum of 270 times per second and can measure up to 40 meters. It has a margin of error of ± 2.5 centimeters over distances longer than one meter (Maulana, Rusdinar, & Priramadhi, 2018). The Lidar sensors make the distance calculation based on the reflection time of the laser beam. Equation 1 shows how to calculate the distance. The value indicated by c represents the speed of the laser beam, the value indicated by t represents the reflection time of the light, and the value indicated by d represents the calculated distance.

$$d = \frac{c \times t}{2} \tag{1}$$

### *2.1.2. HC-SR04 Ultrasonic Sensor*

Ultrasonic distance sensors work with the logic of converting the reflection time of the sound waves into distance information. The HC-SR04 calculates the distance from the time elapsed between sending an 8-speed sound wave in the 40 KHz frequency band and reflection from it and re-reaching it. Ultrasonic distance sensors use a multi-vibrator system, which is a combination of a vibration motor and a resonator. Figure 1 shows the operating logic of HC-SR04 (Açıkel & Gökçen, 2018).

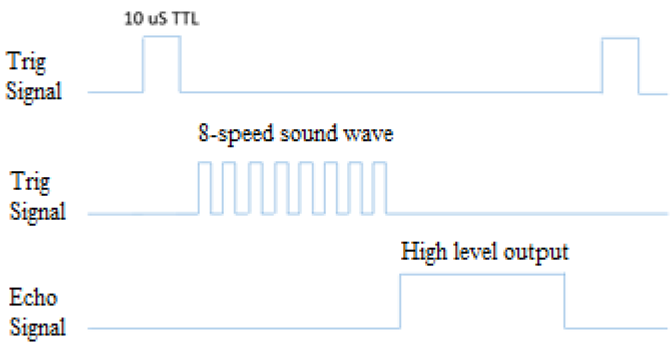


*Figure 1. Working Principle of HC-SR04 (Açıkel, 2018)*

### *2.1.2. Design*

The front and right views of the autonomous robot performing the mapping are shown in Figure 2.

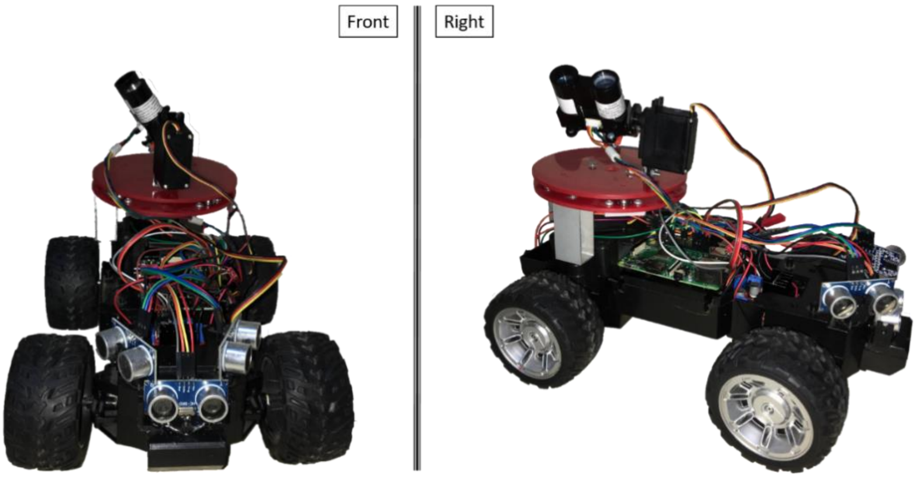


*Figure 2. Autonomous Robot's Views*

In the design of the robot, three ultrasonic sensors were used to escape the obstacle and Lidar Lite V3 was used to collect the map data.

## 2.2. Methods

### *2.2.1. Moving Average Filter*

The moving average filter is a filter that takes a continuous average of a set of values. It is used to improve sensor data, to reduce sharpness in pictures or to remove noise. Moving average filter, a linear filter, is used in this study to minimize errors in a set of measurement data from the lidar sensor. The moving average filter can be shown as in Equation 2 in the continuous time interval.

$$\bar{x}(t) = \frac{1}{T_w}\int_{t-T_w}^{t} x(t)dt \tag{2}$$

$\bar{x}(t)$, is the output value of the system specified in Equation 2. The input value of the equation is $x(t)$. In order to implement the equation of the moving average filter defined in the continuous time interval, a discrete time definition is required. A filtering application with *N* sample can be defined as $T_w = N \times T_s$ using $T_s$ sample time (Golestan, 2013). Equation 3 shows the use of the moving average filter for discrete time application.

$$\bar{x}(k) = \frac{1}{N}\sum_{i=0}^{N-1} x(k-i) \tag{3}$$

$x(k)$, represents the present example and $\bar{x}(k)$, is the output value of the system. The difference of Equation 3 in the Z range has been shown as in Equation 4. The Z range represents the frequency-definition cluster. A discrete expression in the time-definition cluster is converted to the format in the frequency-definition cluster by Z-transformation. (Jury, 1964).

$$\begin{aligned}\bar{X}(z) &= \frac{1}{N}\left(X(z) + z^{-1}X(z) + \cdots + z^{-(N-1)}X(z)\right)\\ &= \left(\frac{1}{N}\sum_{i=0}^{N-1} z^{-1}\right)X(z)\\ &= \frac{1}{N}\frac{1-z^{-N}}{1-z^{-1}}X(z)\end{aligned} \tag{4}$$

In this study, the discrete-time moving average filter equation (Equation 4) was applied to the measurements and the noise has been removed.

### *2.2.2. Calculation of Coordinates*

In order to draw a point in three-dimensional space in a virtual environment, the coordinates of the point are required. The coordinates of the point are calculated with three parameters. These:

• The shortest distance to the origin,

• The angle made in the horizontal axis.

• The angle made in the vertical axis (Üstün, 1996).

Figure 3 shows the parameters required to display a point in the three-dimensional coordinate system. The origin represents the point at which the autonomous robot is located. Angle parameters on the horizontal and vertical axis are taken from the servo motors which provide the movement of the lidar sensor.

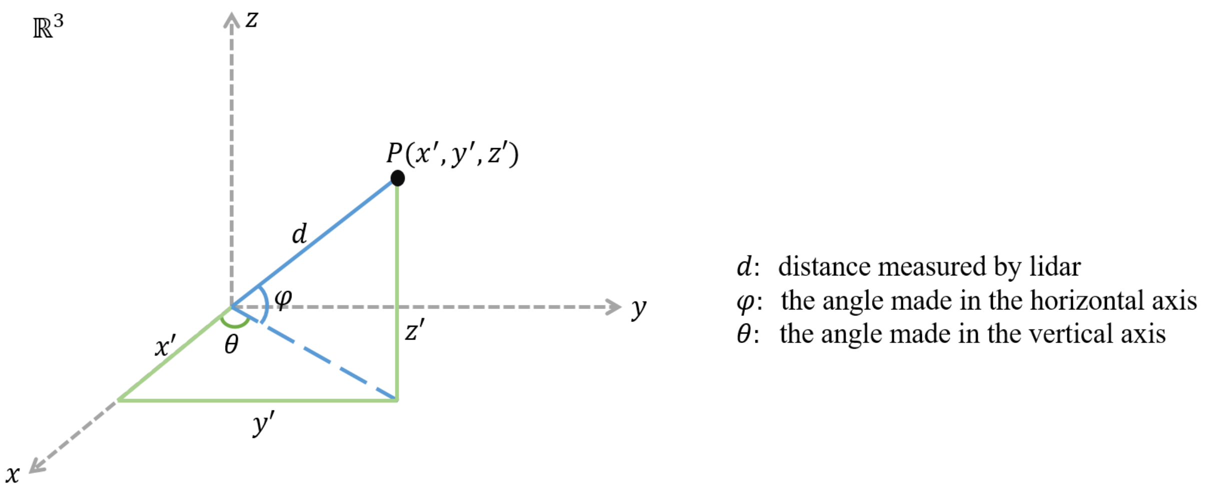


*Figure 3. Showing a Point in a Three-Dimensional Coordinate System*

In order to define a point in three-dimensional space $(x', y', z')$ triplet is used. In Figure 3, $x'$ is defined as the distance to the yz-plane, $y'$ is defined as the distance to the xz-plane and $z'$ is defined as the distance to the xy-plane. In the Equation 5, it is shown that the coordinate calculations made with the parameters obtained from the lidar sensor and servo motors are shown.

$$\begin{bmatrix} x' \\ y' \\ z' \end{bmatrix} = d \times \begin{bmatrix} cos\varphi \times cos\theta \\ cos\varphi \times sin\theta \\ sin\varphi \end{bmatrix} \tag{5}$$

From Equation 5, correlations 6, 7 and 8 are obtained.

$$x' = d \times cos\varphi \times cos\theta \tag{6}$$

$$y' = d \times cos\varphi \times sin\theta \tag{7}$$

$$z' = d \times sin\varphi \tag{8}$$

The Cartesian product in Equation 9, which consists of $x, y, z$ sequential real number triplets are denoted by $\mathbb{R}^3$, and is called the Three-Dimensional Cartesian Coordinate System.

$$\mathbb{R} \times \mathbb{R} \times \mathbb{R} = \{(x, y, z) \mid x, y, z \in \mathbb{R}\} \tag{9}$$

The movements of the autonomous robot affect the condition of the stage. In this case, every action must be reflected on the stage. The projection of the robot movements to the scene was carried out with transformation matrices. The movements of the robot in the $x$ or $y$ axes are reflected to the scene using the translational matrix. Equation 10 shows the translation matrix in the x and y axes (Siciliano, Sciavicco, Villani & Oriolo, 2010).

$$\mathrm{T}_{\mathrm{x,y}} = \begin{bmatrix} 1 & 0 & 0 & \mathrm{t_x} \\ 0 & 1 & 0 & \mathrm{t_y} \\ 0 & 0 & 1 & 1 \\ 0 & 0 & 0 & 1 \end{bmatrix} \tag{9}$$

In addition to the translation process, the rotation of the autonomous robot in the environment must be reflected on the stage. The rotation movements also affect the coordinates of the point. Since the origin of the scene is the point where the autonomous robot is located, the rotation is applied to the origin. The rotational movement of the autonomous robot takes place in the z-axis. The rotation matrix is shown in Equation 11. The angle θ, is the difference between the last angle of the robot and the first angle (Siciliano et al., 2010). A three-axis digital compass sensor is used to obtain the angle difference.

$$R_z(\theta) = \begin{bmatrix} cos\theta & -sin\theta & 0 \\ sin\theta & cos\theta & 0 \\ 0 & 0 & 1 \end{bmatrix} \tag{10}$$

#### *2.2.3. Motion Detection*

Motion detection can be defined as the detection of differences between the initial state of the system and its current state. If the first image of an environment is determined as a background, then any changes in the environment can be easily detected. Motion detection is made by the difference between the image set as a background and the new frames (Bradski & Kaehler, 2008). When the pixel set changes are detected, the pixels in which changes occur can be labelled and movements in the environment can be detected.

In this study, motion detection was made by using pixel group difference method between images using OpenCV Library. The purpose of motion detection is to minimize the noise and error in the environment map by ignoring the dynamic objects inside the environment to be mapped.

## 3. Results and Discussion

Findings from the measurements show that the moving average filter is highly effective on sensor data. For each 1-degree movement of the servo motors, ten distance measurements were made and the measurements were added to the sequence of the moving average filter respectively. The results are shown in Table 1.

*Table 1. Moving Average Filter Effect*

| Iteration | Sensor Data | Moving Average Filter |
|---|---|---|
| **1** | 149,3 | 149,3 |
| **2** | 150,3 | 149,657 |
| **3** | 152,6 | 150,708 |
| **4** | 148,1 | 149,777 |
| **5** | 151,2 | 150,285 |
| **6** | 150,5 | 150,362 |
| **7** | 149,2 | 149,947 |
| **8** | 153,1 | 151,073 |
| **9** | 149,9 | 150,654 |
| **10** | 149,8 | 150,349 |

Table 1 shows the sensor measurements from a point of 150 centimetres and the effect of the moving average filter on these measurements. A 0.2-centimetre error of the final value of the sensor measurements does not mean that the result is healthy in every measurement. The measured distance can be any of the ten measurements in Table 1. Therefore, the data is filtered. The value used for the coordinate account is the last value obtained from the filter. The effect of the moving average filter on the sensor data is shown in Graph 1.

*Graph 1. Moving Average Filter Effect*

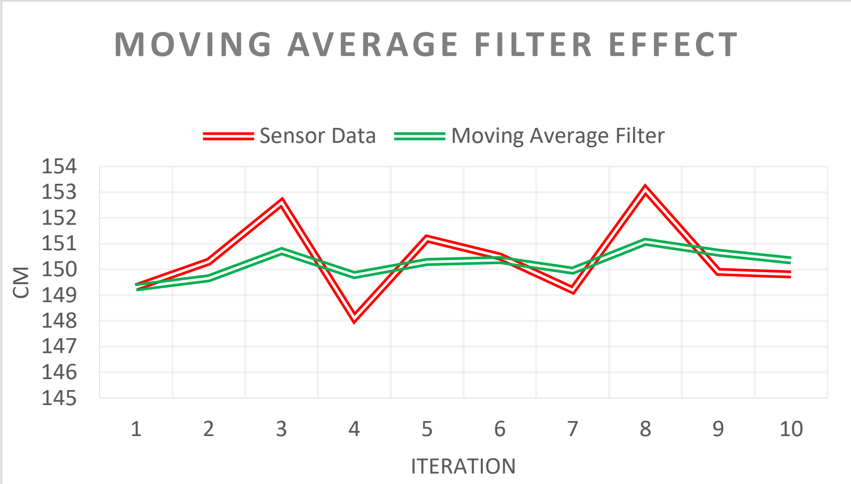


In Graph 1, it is concluded that the amount of sensor data is linearized by moving average filter. After the moving average filter has been applied to all the data, a significant decrease has been observed in the noise. Figure 4 shows the results obtained from the measurements by applying the moving average filter.

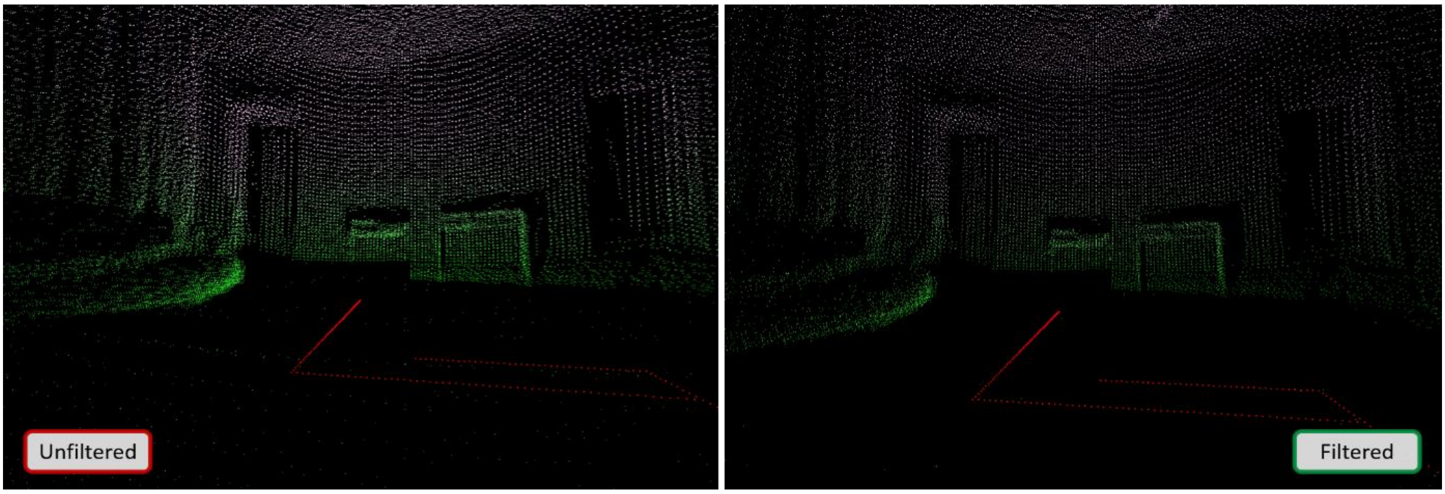


*Figure 4. Applying the Moving Average Filter to All Data*

Figure 4 shows that the moving average filter removes noise from measurement errors and clarifies objects in the map. In Simultaneous localization and mapping studies, have been used Kalman filter and its derivatives like as extended Kalman filter (EKF), which are generally probabilistic methods. Most of the studies with high performance rate have been used EKF. For this reason, EKF have been compared with the moving average filter used in this study. The EKF is a two-stage filter as a motion update and perception update. During motion update, Gauss distribution calculations are performed. During the perception update, the detected movement status is compared with the previous states. The EKF is generally used for filtering nonlinear data. Table 2 and Graph 2 show the measurements taken from a point with a real distance of 263 centimeters and the results obtained after applying filters to these measurements.

*Table 2. Comparison of Moving Average Filter and EKF*

| Iteration | Sensor Data | Moving Average Filter | Extended Kalman Filter |
|---|---|---|---|
| **1** | 258 | 258 | 258 |
| **2** | 260 | 258,714 | 258,947368428092 |
| **3** | 260 | 259,173 | 258,947368428092 |
| **4** | 258 | 258,754 | 258 |
| **5** | 257 | 258,128 | 257,526315789483 |
| **6** | 259 | 258,439 | 258,473684217575 |
| **7** | 265 | 260,782 | 261,315789473619 |
| **8** | 262 | 261,217 | 259,894736842068 |

| | | | |
|---|---|---|---|
| **9** | 256 | 259,354 | 257,052631586010 |
| **10** | 268 | 262,442 | 262,736842112228 |
| **11** | 259 | 261,213 | 258,473684217575 |
| **12** | 264 | 262,208 | 260,842105263102 |
| **13** | 262 | 262,134 | 259,894736842068 |
| **14** | 264 | 262,8 | 260,842105263102 |

*Graph 2. Comparison of Moving Average Filter and EKF*

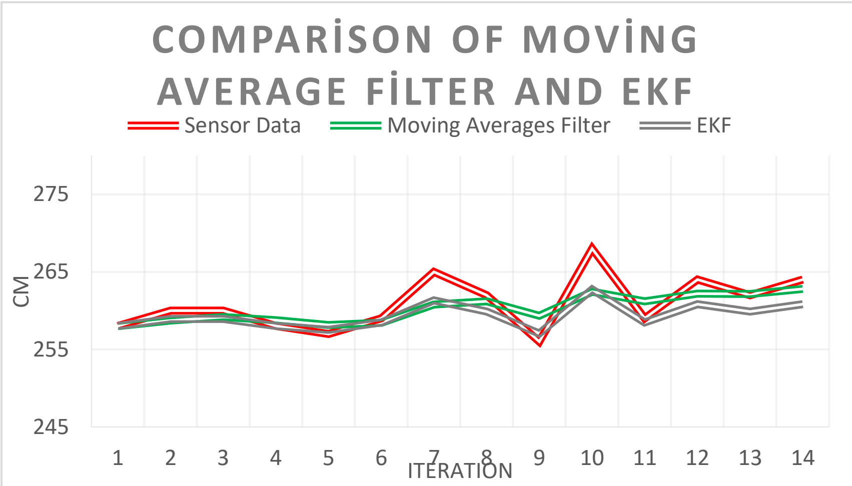


The effect of the moving average filter and the EKF on the environment model data have been shown in Figure 5 and Figure 6. According to the results, it is seen that the moving average filter produces more accurate results. The color scale used in Figures 5 and 6 has been determined by the distance of the points to the origin point. The actual lengths of the displayed values of m,n and h are 250, 370 and 300 centimeters, respectively.

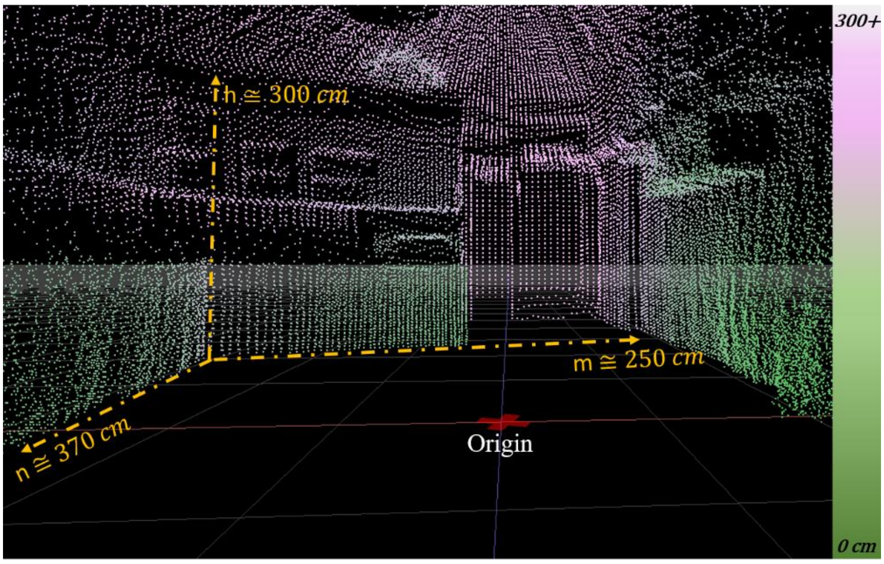


*Figure 5. Moving Average Filter Effect on Environment Model*

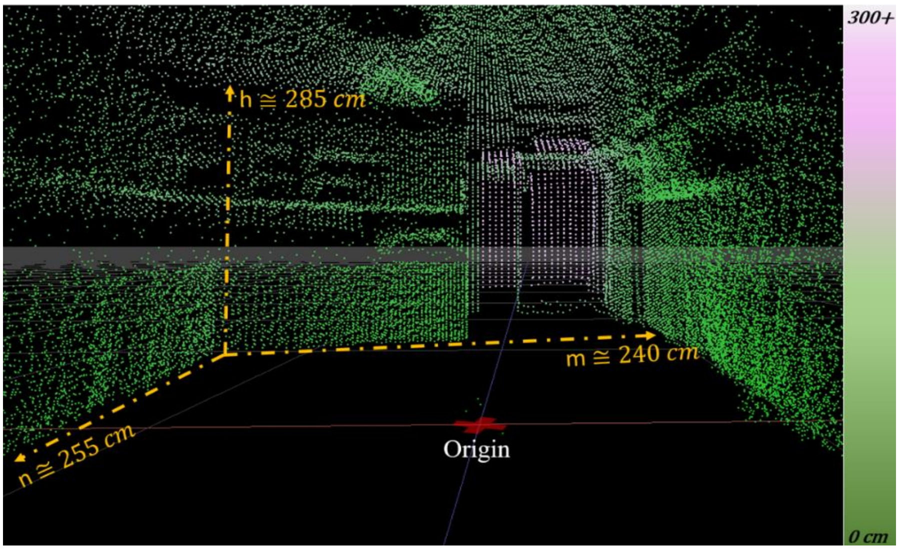


*Figure 6. EKF Effect on Environment Model*

When the filters were compared, has been observed that the EKF-filtered model occupied a lower area in volume, therefore that smaller distance data were generated from the actual data. The moving average filter produced realistic results.

It is important not to create meaningless images when creating a map. In static environments, meaningless images resulting from incorrect measurements are removed with the help of filters. In dynamic environments, only filtering is insufficient. Meaningless lines or objects can be created on the map, although the sensor data is measured correctly. The motion detection algorithm developed by using the OpenCV Library has been added to the autonomous robot in order to avoid nonsense images caused by movements in dynamic environments. If the robot detects a moving object while it is taking its measurement from the environment it is mapped in, it is allowed to pause the measurement process until the environment is restored. Figure 7 shows the detection of moving objects in the environment.


*Figure 7. Detecting Moving Objects*

The movement of autonomous robot is monitored by dc motors with encoder and digital compass sensor. The motion in the environment was transferred to the scene with data from the encoder motors. The rotational movements have been realized by reflecting the angle values obtained from the digital compass sensor to the scene. Figure 8 shows the mapping of a room and the movement of the autonomous robot in the environment.

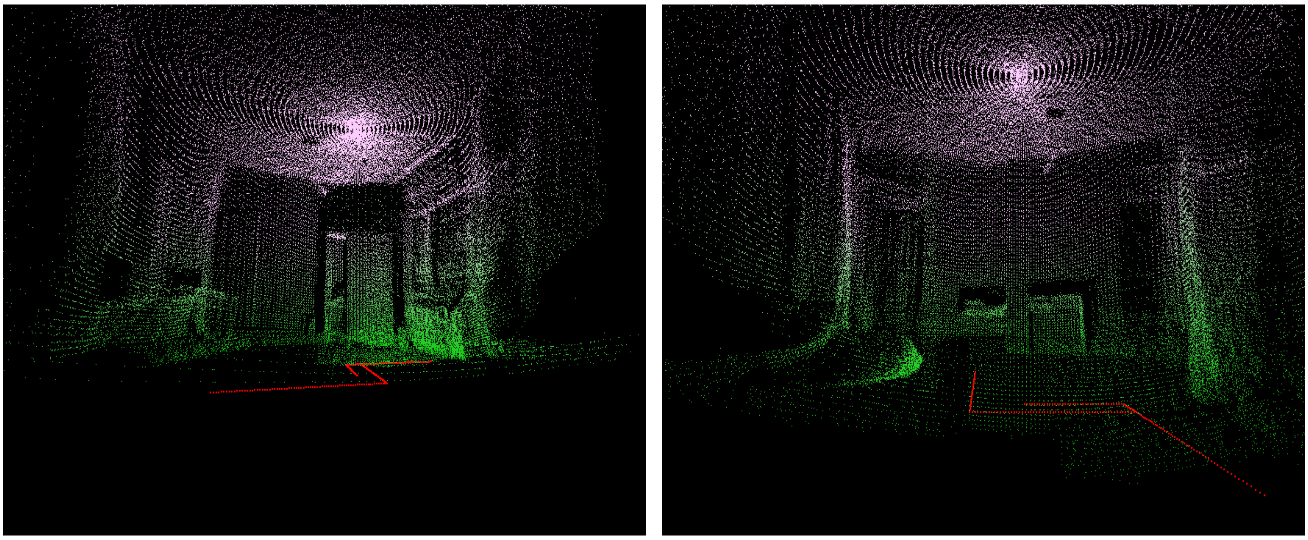

*Figure 8. Three-dimensional Mapping of Environment*

Figure 9 shows the images taken from different perspectives. The red lines are formed by the autonomous robot's own position in the environment as a result of the movements. This room model was obtained from an area of 20 square meters. The designed autonomous robot can scan areas at much larger scales and create a three-dimensional model. Figure 9 shows a three-dimensional model formed by data obtained from a 500 square meter mosque.

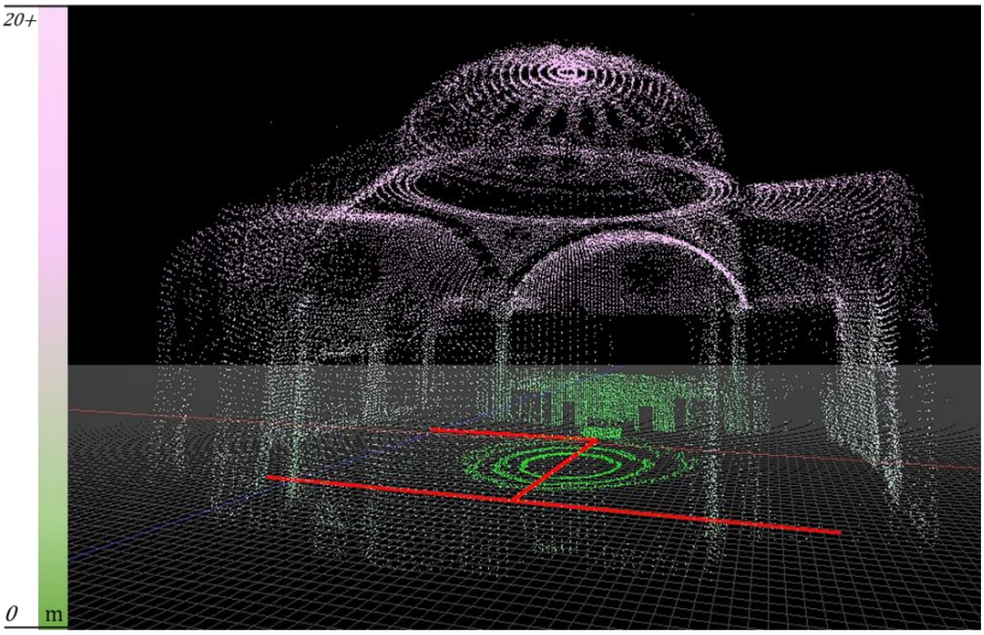


*Figure 9. Three-dimensional Mosque Model*

## 4. Conclusions

In Epilogue to this study, a solution has been developed to prevent the formation of meaningless images in three-dimensional SLAM problems with dynamic motion detection. The success of the moving average filter has been shown to eliminate sensor errors. By taking measurements from three different points of an environment, the meaninglessness of the images in different perspectives was prevented. The movements of the autonomous robot have been accurately analysed to prevent image shifts during the measurements.

## References

Açıkel, S. & Gökçen A. (2018). Two-dimensional environmental mapping and route tracking by using lidar in otonom robots. IV. INES Internatıonal Academic Research Congress (INES - 2018), Antalya.

Altuntaş, N., Uslu, E., Çakmak, F., Amasyalı, M. F., & Yavuz, S. (2017, October). Comparison of 3-dimensional SLAM systems: RTAB-Map vs. Kintinuous. In Computer Science and Engineering (UBMK), 2017 International Conference on (pp. 99-103). IEEE.

Ankışhan, H., & Efe, M. (2010). Kalman filter approaches for simultaneous localization and mapping. DÜMF Engineering Journal, 1(1), 13-20.

Bradski, G., & Kaehler, A. (2008). Learning OpenCV: Computer vision with the OpenCV library. "O'Reilly Media, Inc.",(pp. 265-271)

Carlone, L., Tron, R., Daniilidis, K., & Dellaert, F. (2015, May). Initialization techniques for 3D SLAM: a survey on rotation estimation and its use in pose graph optimization. In Robotics and Automation (ICRA), 2015 IEEE International Conference on (pp. 4597-4604). IEEE.

Dissanayake, M. G., Newman, P., Durrant-Whyte, H. F., Clark, S., & Csorba, M. (2000). An experimental and theoretical investigation into simultaneous localisation and map building. In Experimental robotics VI (pp. 265-274). Springer, London.

Durrant-Whyte, H., & Bailey, T. (2006). Simultaneous localization and mapping: part I. IEEE robotics & automation magazine, 13(2), 99-110.

Fowler, R. A. (2000). The lowdown on LIDAR. Earth Observation Magazine, 9(3), 5.

Golestan, S., Ramezani, M., Guerrero, J. M., Freijedo, F. D., & Monfared, M. (2013). Moving average filter based phase-locked loops: Performance analysis and design guidelines. IEEE Transactions on Power Electronics, 29(6), 2750-2763.

Graff, K. F. (1981). A history of ultrasonics. In Physical acoustics (Vol. 15, pp. 1-97). Academic Press.

Hosseinzadeh, M., Li, K., Latif, Y., & Reid, I. (2018). Real-Time Monocular Object-Model Aware Sparse SLAM. arXiv preprint arXiv:1809.09149.

Jury, E. I. (1964). Theory and Application of the z-Transform Method (pp. 176-179).

Kurt, Z. (2007). Development of intelligent algorithms for simultaneous positioning and mapping. (Doctoral dissertation, Yıldız Technical University, Institute of Science and Technology, Istanbul).

Lee, K., Ryu, S. H., Nam, C., & Doh, N. L. (2018). A practical 2D/3D SLAM using directional patterns of an indoor structure. Intelligent Service Robotics, 11(1), 1-24.

Maulana, I., Rusdinar, A., & Priramadhi, R. A. (2018). Application of Lidar for Mapping and Navigation in Closed Environments. eProceedings of Engineering, 5(1).

Ramli, M. F. B., Shamsudin, S. S., & Legowo, A. (2017). Obstacle Detection Technique Using Multi Sensor Integration for Small Unmanned Aerial Vehicle. Indonesian Journal of Electrical Engineering and Computer Science, 8(2), 441-449.

Rusu, R. B., Marton, Z. C., Blodow, N., Dolha, M., & Beetz, M. (2008). Towards 3D point cloud based object maps for household environments. Robotics and Autonomous Systems, 56(11), 927-941.

Siciliano, B., Sciavicco, L., Villani, L., & Oriolo, G. (2010). Robotics: modelling, planning and control. Springer Science & Business Media.

Thrun, S. (2002). Robotic mapping: A survey. Exploring artificial intelligence in the new millennium, 1(1-35), 1.

Üstün, A. (1996). Datum conversions. (Master Thesis, Yıldız Technical University, Institute of Science and Technology, Istanbul).